Table S1. Related to Experimental Procedures

Characterization of SAC polarity.

Figure[1]	Experiment[2]	Control[3]	Adapted[4]	Both[5]
1D	Dorsal On SACs	12	13	9
1D	Off SAC	9	9	9
2B	Ventral On SACs	11	12	6
3H	PSAM	4	6	2
4F	Cx36 KO	11	11	7

Pharmacological manipulations

Figure[1]	Experiment[2]	Adapted[4]	Drug[6]	Both[7]
4B	L-AP4	6	6	4
4C	Gabazine	6	6	4
4C	Strychnine	6	6	6
4C	TPMPA	2	4	2
4E	L-AP4	5	5	5
4F	MFA		10	

[1] Figure in which the experiment with the sample sizes listed is presented.
[2] Specific experiment that contained the sample sizes described. Mentions either the class of cells being recorded from or the pharmacological neurotransmitter blocker added.
[3] Refers to sample size of cells recorded before repetitive stimulation in control conditions.
[4] Refers to sample size of cells recorded after repetitive stimulation took place.
[5] Refers to sample size of cells recorded in paired conditions both before and after repetitive stimulation.
[6] Refers to sample size of cells recorded during treatment with pharmacological blocker in the stimulated state.
[7] Refers to sample size of cells recorded in paired conditions after repetitive stimulation and in pharmacological blocker (drug).

Figure S1
Vlasits

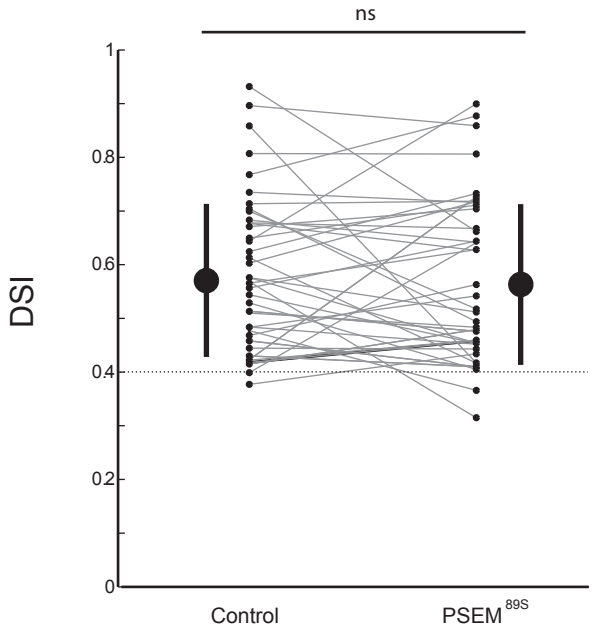

Figure S2
Vlasits

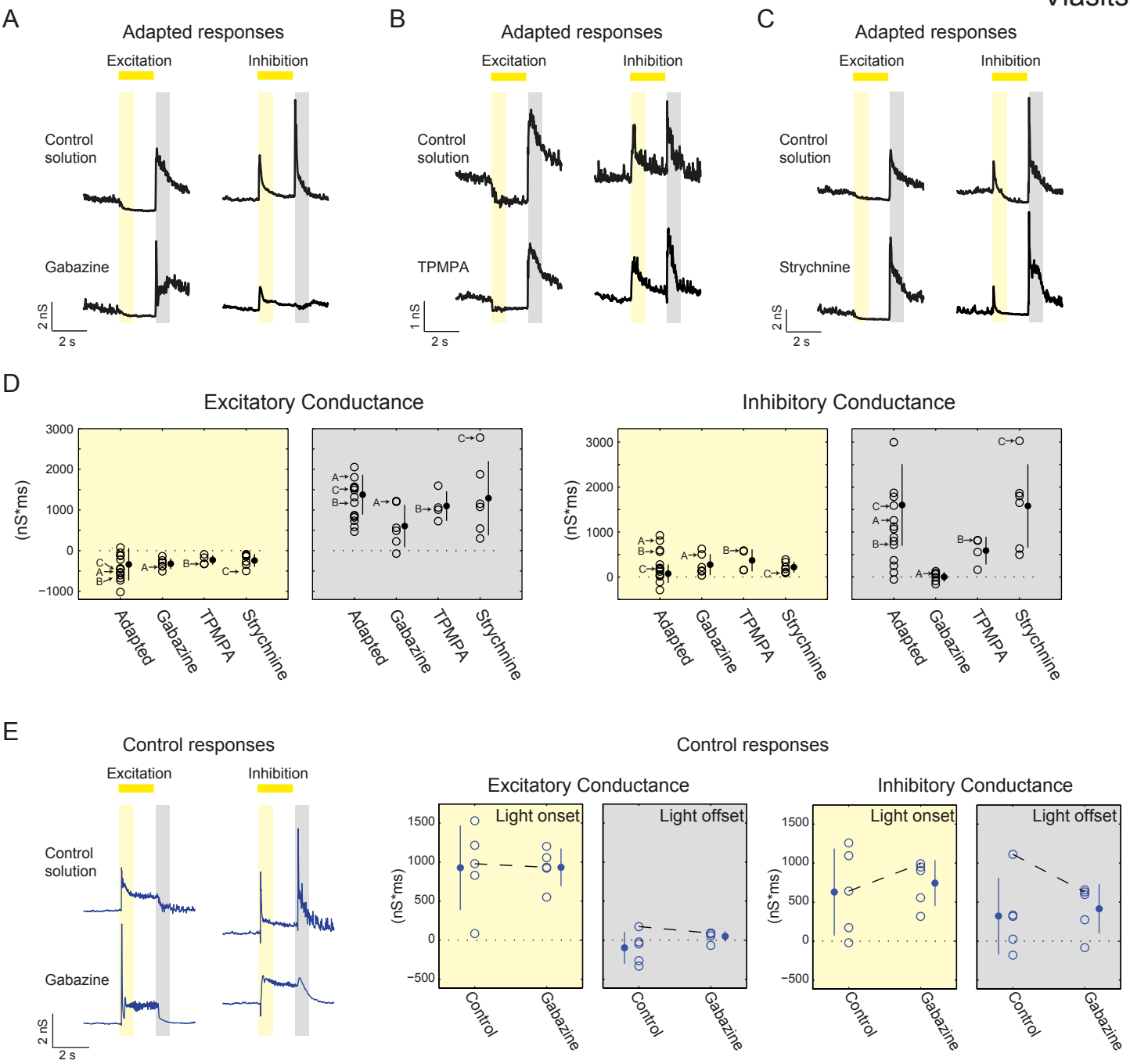

Figure S3
Vlasits

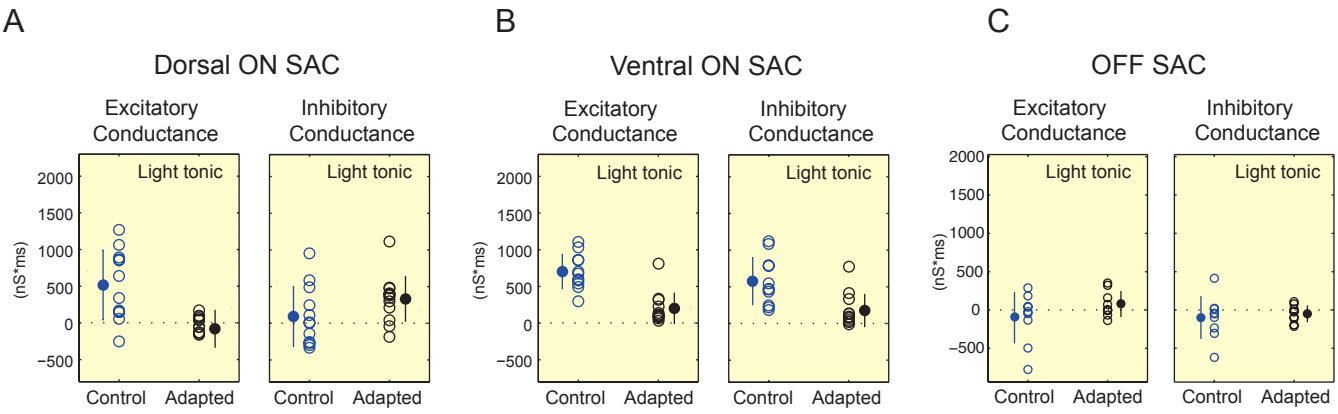

Figure S4
Vlasits

A

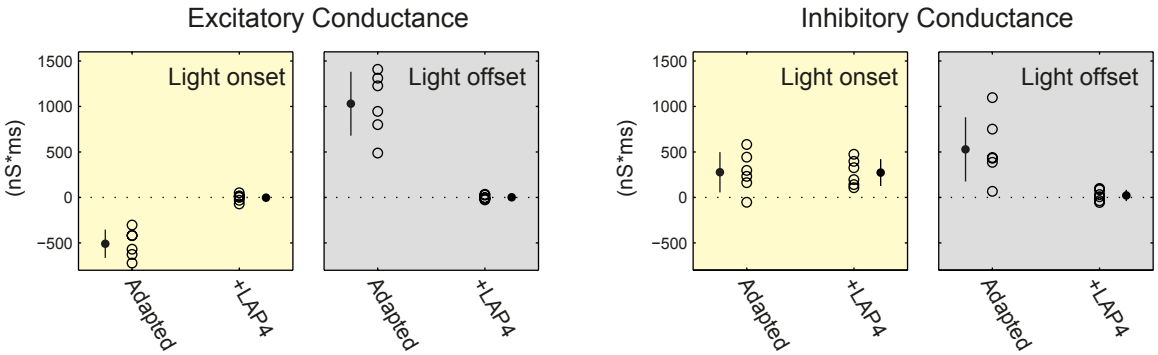

B

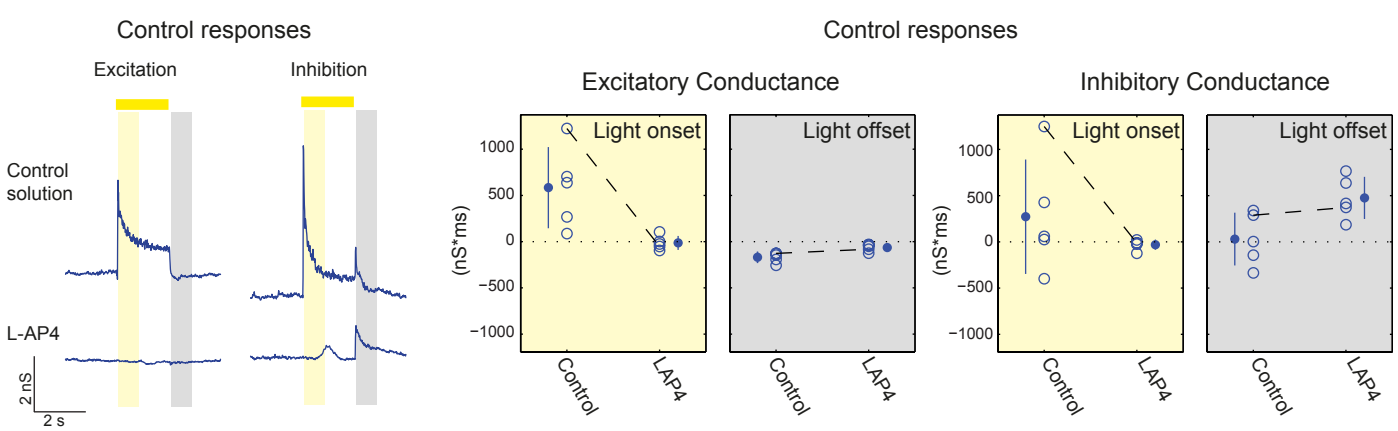

Figure S5
Vlasits

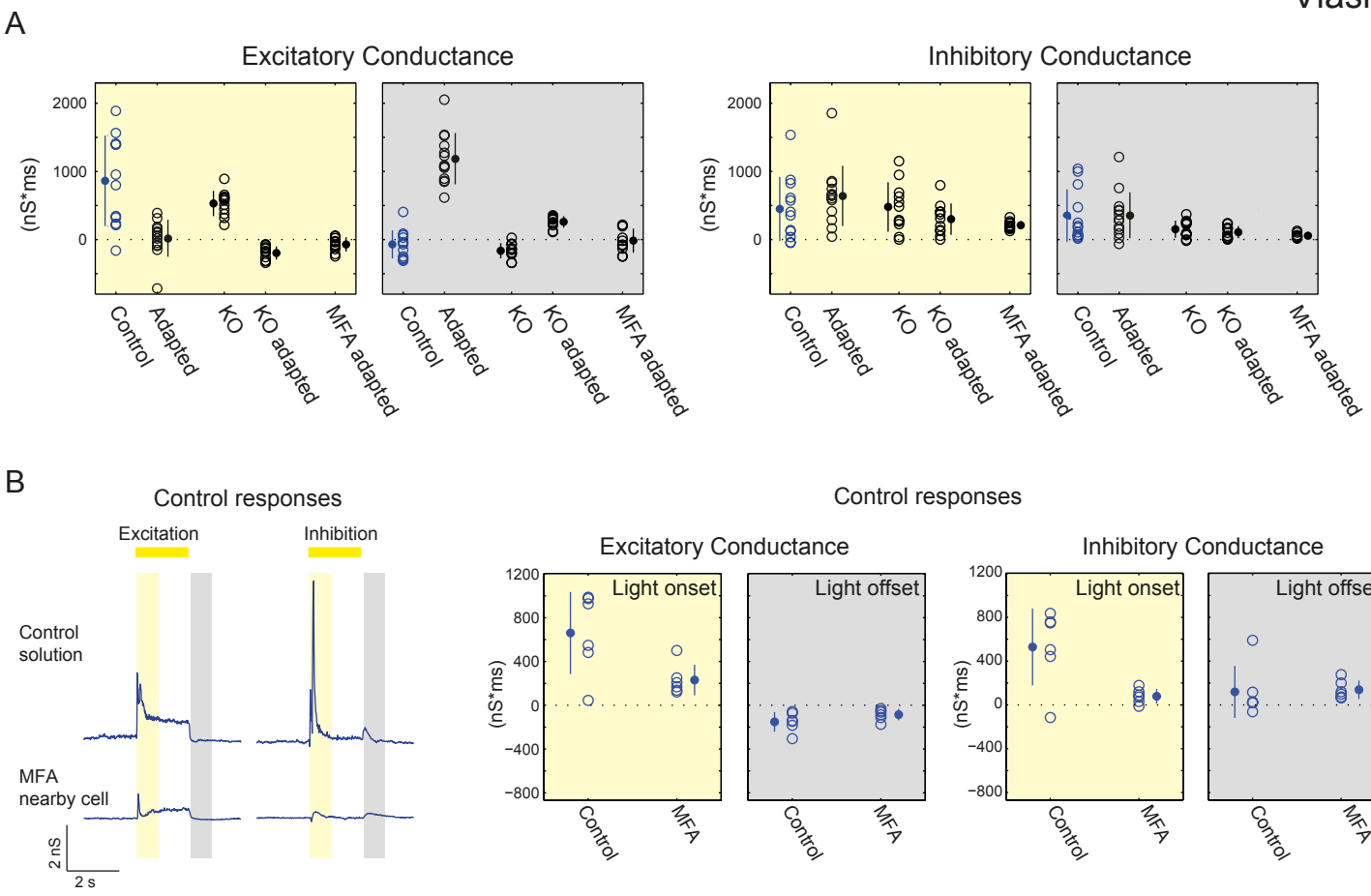

Figure S6
Vlasits

A

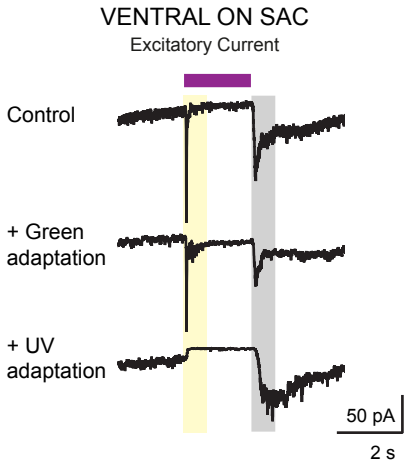

B

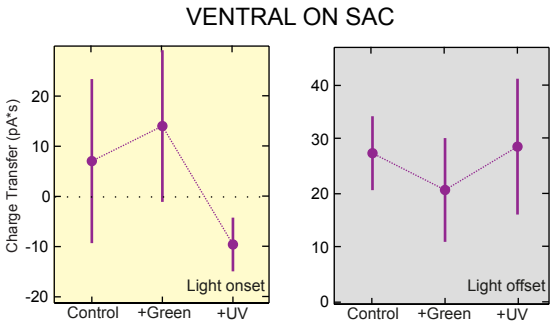

Supplemental Figure Legends

Figure S1. (Related to Figure 1) PSEM^{89S} has no effect on direction selective tuning of DSGCs in wild type mice.

Effect of PSEM^{89S} on the direction selectivity index (DSI) of On (red) and On-Off (blue) DSGCs (n = 46 cells, small black circles) in 4 retinas from wild type mice, which were not infected with PSAM virus. DSI was determined using 2-photon calcium imaging as described in Figure 1. Large circles are group means, error bars are SD, dotted line indicates the threshold DSI for defining a cell as a DSGC (DSI > 0.4).

Figure S2. (Related to Figure 3) Conductance analysis of control and adapted responses in the presence of inhibitory blockers.

(A-C) The excitatory and inhibitory conductance at light onset and light offset for adapted On-SACs in control solution and in 5 μM Gabazine (A), 50 μM TPMPA (B) or 1 μM Strychnine (C). Conventions are as in Fig. 2C.

(D) The excitatory (left) and inhibitory (right) integrated conductance at light onset and light offset for adapted On-SACs in control solution and after application of 5 μM gabazine, 1 μM strychnine, or 50 μM TPMPA. Conventions are as in Fig. 2E. Arrows indicate conductances of example cells in A-C.

(E) Left: the excitatory and inhibitory conductance at light onset and light offset for unadapted On-SACs in control solution and in 5 μM Gabazine. Conventions are as in Fig. 2C. Right: The excitatory (left) and inhibitory (right) integrated conductance at light onset and light offset for unadapted On-SACs in control solution and after application of 5 μM Gabazine. Conventions are as in Fig. 2E.

Figure S3. (Related to Figures 2 and 4) Tonic excitatory conductances are reduced in On and Off-SACs after adaptation.

The light response had two components – a fast transient component followed by a slower tonic component. We independently quantified the changes in the tonic response following repetitive stimulation by integrating over the period between 1050–1850 ms after light onset for both On- and Off-SACs. The results mirrored the results at light onset, with both dorsal and ventral On-SACs losing the tonic On response after repetitive stimulation.

Excitatory and inhibitory conductances from dorsal On-SACs (A), ventral On-SACs (B) and Off-SACs (C). The time periods for calculating the tonic integrated conductance was 1050 – 1850 ms after light onset. Blue data = controls (before adaptation), black data = adapted cells. Empty circles are conductances in individual cells. Mean values are represented by the filled circles, error bars = standard deviation.

Figure S4. (Related to Figure 5) Conductance analysis of control and adapted responses in the presence of L-AP4.

(A) The excitatory (left) and inhibitory (right) integrated conductance at light onset and light offset for adapted On-SACs in control solution and in 5 μM L-AP4. Conventions are as in Figure 2E.

(B) Left: the excitatory and inhibitory conductance at light onset and light offset for unadapted On-SACs in control solution and in 5 μM L-AP4. Conventions are as in Fig. 2C. Right: The excitatory (left) and inhibitory (right) integrated conductance at light

onset and light offset for unadapted On-SACs in control solution and after application of 5 μM L-AP4. Conventions are as in Fig. 2E.

Figure S5. (Related to Figure 6) Conductance analysis of control and adapted responses in Cx36 KOs and in MFA.

(A) The excitatory (left) and inhibitory (right) integrated conductance at light onset and light offset for On-SACs in control solution and after adaptation in WT and Cx36 KO retinas, as well as in WT retinas in the presence of 100 μM MFA. Conventions are as in Fig. 2E.

(B) Left: the excitatory and inhibitory conductance at light onset and light offset for unadapted On-SACs in control solution and in 100 μM MFA. Conventions are as in Fig. 2C. Example shown is from two nearby cells. Right: The excitatory (left) and inhibitory (right) integrated conductance at light onset and light offset for unadapted On-SACs in control solution and after application of 100 μM MFA. Conventions are as in Fig. 2E.

Figure S6. (Related to Figure 7) SACs in Ventral Retina Switch Polarity after Adaptation with UV Light.

To evaluate whether SACs in the ventral retina can switch their polarity, we measured the response to 2 s stationary spots of “UV” light before and after adaptation. Note these experiments were not carried out on a two-photon microscope and therefore the retina piece was exposed to several seconds of bright green light prior to starting the protocol.

First, we recorded the spot responses to UV light (Control). Then, to completely saturate the rods, we exposed the cells to steady green light for 10 s. We then recorded the spot response to UV light. Finally, we adapted the cells to steady UV light for 7 min before evaluating the response to UV spots again. We found that On-SACs in the ventral retina exhibited both an On and Off response to UV light spots before adaptation (Fig. S6). This initial response was not affected by adaptation with Green light. Subsequent adaptation with UV light led to a loss of the On response, resulting in a spot response similar in kinetics to the adapted responses we recorded in adapted On-SACs in the dorsal retina (see Fig. 2). These data are consistent with the model proposed in Figure 7 – that the Off response is 1) loss of a rod and cone-mediated On light response and 2) mediated by cone photoreceptors via surround inhibition of rods.

(A) Voltage clamp recording from an On-SAC in ventral retina showing excitatory current (Holding Potential = -72 mV) in response to a 2 s stationary spot stimulus with UV-wavelength light (purple bar) in control conditions and following exposure to 10 s of Green light ("Green adaptation") followed by exposure to 7 min of UV light ("UV adaptation"). Yellow and grey bars indicate the time periods used for analysis in (B). Traces are averages of 5 sweeps.

(B) Charge transfer (averaged over five sweeps) of the excitatory current during light onset (yellow) and light offset (grey) for ventral On-SACs in control conditions and following exposure to 10 s of Green light ("Green") followed by exposure to 7 min of UV light ("UV"). Error bars = SD. N = 5 cells from 2 mice.

Methods: Visual stimuli were transmitted through a 60x objective (Olympus LUMPlanFl/IR 60/0.90W) on a fixed stage microscope (Olympus, BX61WI) using a Xenon Arc Lamp. “UV” and “Green” stimulations were produced using neutral density filters along with a Fura2 filter cube (measured excitation spectrum: 375-400 nm) and YFP filter cube (measured excitation spectrum: 490-510 nm), respectively. Light intensity was 2.9 x 10^6 R*/rod/s (1.54 x 10^7 photons/μm^2/s) for “UV” and 2.28 x 10^8 R*/rod/s (2.28 x 10^8 photons/μm^2/s) for “Green” stimulation. Importantly, the “UV” stimulation provided a 5.38 x 10^6 sOpsin*/sCone/s intensity and therefore primarily activated sOpsin. An aperture in the light path was used to limit light spots to ~220 μm in diameter. To target cells for electrophysiology, GFP immunofluorescence was imaged with a <1 s exposure using a GFP filter cube. The duration of light stimuli used to adapt ventral On-SACs was determined by comparing the light intensity to the light intensity of the OLED used for light adaptation elsewhere and adjusting the duration so that cells were exposed to roughly the same number of total photons. Electrophysiology data acquisition was conducted as described in Experimental Procedures.

Extended Experimental Procedures

Animals

All animal procedures were approved by the UC Berkeley Institutional Animal Care and Use Committee and conformed to the NIH Guide for the Care and Use of Laboratory Animals, the Public Health Service Policy, and the SFN Policy on the Use of Animals in Neuroscience Research. Adult mice (P21-P40) of either sex were anesthetized with isoflurane and decapitated. Retinas were dissected from enucleated eyes under infrared illumination and orientation was determined based on stereotyped landmarks in the choroid as described previously (Wei et al., 2010). For calcium imaging of DSGCs, isolated retinas were mounted photoreceptor layer side down on a ring-supported hydrophilic PTFE membrane (Millipore) (Ivanova et al., 2013). For whole cell recordings, isolated retinas were mounted over a 1-2 mm^2 hole in filter paper (Millipore) with the photoreceptor layer side down. Mounted retinas were stored in oxygenated Ames' media (US Biological) in the dark at room temperature prior to imaging or recording. Retinas from C57BL/6 mice were used for calcium imaging. To target SACs for whole cell recordings, we used two mouse lines that express fluorescent protein in starburst amacrine cells. On- and Off-SACs were targeted with *mGluR2-GFP* mice that contain a transgene insertion of interleukin-2 receptor fused to GFP under control of the mGluR2 promoter (Watanabe et al., 1998). On SACs were also targeted with *ChAT-Cre/TdTomato* mice generated by crossing a mouse in which IRES-Cre recombinase was knocked in downstream of the endogenous choline acetyltransferase gene (Ivanova et al., 2010) (Chat-cre) with a mouse line containing a loxP-flanked STOP cassette upstream of the tdTomato gene (B6.129S6-$ChAT^{tm1(cre)lowl}$/J × B6.129S6-

Gt(ROSA)26Sor$^{tm9(CAG-tdTomato)Hze}$/J, Jackson Labs). Connexin-36 knockout mice in which the *Cx36* coding sequence was replaced by a LacZ-IRES-PLAP reporter cassette were a generous gift from David Paul at Harvard Medical School (Deans et al., 2002).

Simultaneous Calcium Imaging and Visual Stimulation of DSGCs

The calcium dye Oregon Green 488 BAPTA-1 hexapotassium salt (OGB-1, Invitrogen) was electroporated using the ECM-830 Square Wave electroporation System (BTX Harvard apparatus) to uniformly label neurons within the ganglion cell layer of retinas mounted on ring-supported hydrophilic PTFE membranes. 8 µl of Ames's medium was placed on the lower caliper electrode, the mounted retina was placed over the lower electrode, and 5 µl of OGB-1 (5mM) was directly pipetted onto the tissue. Based on (Briggman and Euler, 2011), the following parameters were applied: ten 13-14 V (top electrode, on ganglion cell layer side), 10-ms-pulse-width, 1-Hz-pulse-frequency squarewave pulses. The distance between the two electrodes was fixed at 1.5 mm. The time to transfer the tissue to the recording chamber after electroporation was < 20 s. All of these procedures were performed under dim red illumination.

Two-photon fluorescence images were obtained with a modified movable objective microscope (MOM) (Sutter Instruments) using a 60x objective (Olympus LUMPlanFLN/IR360/1W). Two-photon excitation of the green calcium dye OGB-1 was evoked with an ultrafast pulsed laser (Chameleon Ultra II; Coherent) tuned to 800 nm. The microscope system was controlled by ScanImage software (www.scanimage.org). Scan parameters were [pixels/line * lines/frame (frame rate in Hz)]: [256 * 256 (1.5)], at

2 ms/line. This MOM was equipped with through-the-objective light stimulation and two detection channels for fluorescence imaging. Visual stimuli were generated using MATLAB software and projected to the photoreceptor layer using a modified video projector (HP AX325AA Notebook Projector Companion; HP) displaying a UV light (single LED NC4U134A, peak wavelength 385 nm; Nichia). The intensity for the UV stimulus was 1.81 x 10^4 R*/cone/s. To decrease the noise entering the photon multiplier tubes due to the UV stimulation, we placed an emission filter (HQ535/50m-2P-18°AOI; Chroma Technology) in front of the green detection channel and a GG475 Schott glass filter (Chroma Technology) in front of the whole detector path. We used two kinds of stimuli: a series of flashed spots (231 µm diameter) and a bar (200 * 350 µm) moving in eight different directions across the field of view at 0.5 mm/s. Each direction was repeated three times. In both cases, the stimulus had a positive contrast (bright on darker background).

PSAM-PSEM neuronal silencing

The PSAML141F,Y115F:GlyR-IRES-GFP construct was subcloned from rAAV-syn::FLEX-rev::PSAML141F,Y115F:GlyR-IRES-GFP (Addgene #32481) into an AAV serotype 2 virus backbone (Dalkara et al., 2013). Vectors were packaged with the 7m8 capsid variant (Dalkara et al., 2013) according to methods in (Flannery and Visel, 2013). For viral injections, P6-8 ChAT-Cre mice (Ivanova et al., 2010) were anaesthetized with 3% isoflurane/2% O_2. After applying lidocaine to the eyelid, the eyelid was opened with fine forceps, and an entry hole was made at the limbus with a sharp 30 gauge needle. 1-1.5µL of 10^{13} vg/mL 7m8-AAV2::FLEX-rev::PSAML141F,Y115F:GlyR-IRES-GFP was

then intravitreally injected through this opening using a Borghuis Syringe (borghuisinstruments.com) and eyes were treated with opthalamic antibiotic drops before being returned to the cage. Light response of animals was assessed ≥3 weeks post-injection. To activate PSAM, 2mM PSEM^{89S} (kind gift of Scott Sternson) stocks in dH_2O were diluted 1:100 in Ames' media. Retinas were perfused with 20μM PSEM^{89S} for at least 15 minutes prior to assessing PSAM activation (Fig. 3A). To measure the effect of PSEM^{89S} on the input resistance of On-SACs, we performed voltage clamp recordings on PSAM-expressing cells by targeting GFP-positive cells using 2-photon microscopy as described below. Cells were stepped to at least two holding potentials to create an I-V curve of the holding current. Then, we calculated the input resistance from the slope of the linear fit to the I-V curve. All linear fits had R-squared > 0.94.

Retinal Histology

Whole mount retinas were fixed in 4% PFA for 3 hours at 4^{o}C, then washed 5 times with PBT (.1% Triton-X 100 in PBS), and left in block solution (4% bovine serum albumin (Sigma) in PBT) for 4 hours at 4^{o}C. Retinas were then incubated in primary antibody (1:250 Goat anti-ChAT, Millipore, AB144P and 1:1000 rabbit anti-GFP, Life Technologies, A11122) diluted in block solution for 4 days at 4^{o}C. After washing retinas with PBT (3 times, 10 minutes) and block solution (2 times, 10 minutes), they were incubated in secondary antibody (1:1000 donkey anti-Rabbit Alexa Flour 488, Life Technologies; 1:1000 donkey anti-goat Alexa Fluor 568, Invitrogen) diluted in block solution overnight at 4^{o}C. After washing 5 times with PBT and twice with PBS, retinas were mounted and coverslipped with Vectashield (Vector Laboratories).

Two-photon Targeted Electrophysiology

Retinas mounted on filter paper were placed under the microscope and perfused with oxygenated (95% O_2 – 5% CO_2), bicarbonate-buffered Ames' media at 32-34°C. To avoid bleaching the photoreceptors, fluorescently labeled retinal cells were targeted for whole cell recordings using two-photon microscopy at 920 nm to visualize fluorescence; and infrared illumination (>800 nm) to visualize cell morphology and guide the patch pipette (Wei et al., 2010). The inner limiting membrane above the targeted fluorescent cell was removed using a glass pipette before targeting a new pipette for recording. For whole cell voltage clamp recordings, borosilicate glass electrodes pulled to a 5-7MΩ tip were filled with an internal solution containing (in mM): 110 CsMeSO3, 2.8 NaCl, 4 EGTA, 5 TEA-Cl, 4 adenosine 5'-triphosphate (magnesium salt), 0.3 guanosine 5'-triphosphate (trisodium salt), 20 HEPES, and 10 phosphocreatine (disodium salt) with pH 7.2. For recordings from Off-SACs, 0.03 mM Alexa Fluor 594 hydrazide (Life Technologies, #A-10438) was included in internal solution for collecting 2-photon images of dendritic morphology after the visual stimulation protocol was complete. To target On-SACs in connexin-36 knock-out mice, we filled cells with small, round somas (Petit-Jacques et al. 2005) with Alexa Fluor 594 in the internal solution and imaged the dendritic morphology using a 2-photon microscope to determine cell identity before recording. A gigaohm seal was obtained before breaking in. Data were acquired at 10 KHz and filtered at 2 KHz with a Multiclamp 700A amplifier (Molecular Devices) using pCLAMP 10 recording software and a Digidata 1440 digitizer. The series resistance was measured during each sweep of the recordings using a -5 mV step and series resistance compensation was completed offline as described below in *Data Analysis*.

For measuring synaptic currents, we recorded 5 sweeps at 4 different holding potentials (-72 mV, -32 mV, -12 mV and +8 mV) and averaged across the sweeps. For Fig. 3B-C, 4E-F and Fig. 5F-G, currents were recorded at only one holding potential (-72 mV). All holding potentials reported here are after correction for the junction potential (-12 mV). For pharmacology experiments, the following concentrations of neurotransmitter blockers were included in the Ames' media (in μM): 5 L-AP4, 5 gabazine, 100 MFA, 1 strychnine, or 50 TPMPA. The protocol for pharmacology experiments was the following: (1) perform repetitive stimulation, (2) record in adapted condition, (3) wash in pharmacological agent, then wait 10 min before recording drug condition. In some cases, we recorded from an adapted SAC in the control media and then recorded from a nearby SAC in the drug-containing media. For Figure S2, S4 and S5, unstimulated responses to drug application were recorded 10 minutes after pharmacological agents were added.

Fluorescence image acquisition

For Fig. 1A, confocal images of immunostained whole mount retinas were taken with a Zeiss inverted AxioOberver Z1 with a LSM 710 confocal scanhead using a 20x/0.8 Plan-Apochromat air objective and 488nm and 561nm laser lines. Z-stacks were acquired with a 0.86μm step size using ZEN software.

To image the dendritic morphology of Off-SACs (Fig. 2) and verify On-SAC identity in Cx36 KO mice (Fig. 6 and Fig. S5), fluorescence images of Alexa-594 dye-filled SACs were collected using a custom-modified two-photon microscope ((Wei et al., 2010); Fluoview 300, Olympus America Inc.) at 810 nm. Images were collected over the

depth of the ganglion cell layer, inner plexiform layer, and inner nuclear layer at 1 μm increments. For the image of Off-SAC in Fig. 2A brightness and contrast were adjusted to more easily visualize the dendritic morphology.

Visual Stimulation of SACs

Visual stimuli were transmitted through a 60x objective (Olympus LUMPlanFL N/60x /1.00W) using an OLED display mirroring a monitor displaying custom stimuli created using MATLAB software with the Psychophysics Toolbox as described previously (Huberman et al., 2009). The emission spectrum of the OLED was cut below 470 nm and therefore did not stimulate the UV-sensitive ventral cones (Wang et al., 2011). Display images were centered on the soma of the recorded cell and were focused on the photoreceptor layer. All experiments were carried out in the photopic light range: background light intensity of the OLED was 1.15 x 10^4 R*/rod/s, which we defined as the “light off” or “light offset” period. Light spot stimuli consisted of a 225 μm diameter white spot with intensity 2.2 x 10^5 R*/rod/s presented for 2 s unless otherwise stated. For measuring synaptic currents, the light spot was presented 5x at 6 or 8 s intervals at the 4 different holding potentials listed above. For the repetitive stimulus, we used a protocol that efficiently reversed directional preference of On-Off direction selective ganglion cells (Rivlin-Etzion et al., 2012). The stimulus consisted of symmetric drifting gratings with 225 μm/cycle, 4 cycle/s, corresponding to 30 deg/s. The light intensity of the gratings was at 100% contrast for the OLED display; the mean intensity (grey) was 1.15 x 10^5 R*/rod/s. First, gratings drifting in 8 different directions were presented for 3 s either 4x or 8x in a row; next gratings drifting in the nasal direction were presented for

40 s followed by 40 s drifting in the temporal direction; finally we repeated the stimulation of gratings in 8 directions. For Fig. 4E-F, bouts of gratings were alternated with light spot stimuli at -72 mV to measure the excitatory current during the repetitive stimulation. For Fig. 5F-G, the duration of the light flash was varied and the light was flashed 5x times in a row for each duration. To verify that changes in conductance of adapted SACs do not emerge as a result of prolonged whole-cell recordings, we stimulated a subset of cells in each experiment before attaching onto them (Table S1).

Data analysis

Data analysis was performed in MATLAB (MathWorks), ImageJ, and IgorPro (WaveMetrics). Conductance analysis to determine excitatory and inhibitory synaptic inputs was performed in MATLAB using the algorithm described in Taylor & Vaney (Taylor and Vaney, 2002). Briefly, sweeps at each holding potential were downsampled by calculating the average current in 10 ms bins and then downsampled sweeps were averaged. The baseline holding current (I_h) was defined as the average current during the 2 s before the light flash and was subtracted from each average trace. We compensated for the series resistance (R_s) by measuring the series and input resistance (R_{in}) from a -5 mV pulse at the end of each trace. Because SACs have a large amount of spontaneous activity at rest (Fig. 5B-E), we selected the values to use for series resistance compensation from the holding potential with the least amount of spontaneous activity as determined by visual inspection offline for each cell. We used the following equations for compensation of the recorded current (I_m) and the holding potential (V_h):

(1) $I_{m,compensated} = I_m * \frac{R_{in}+R_s}{R_{in}}$

(2) $V_{h,compensated} = V_h - I_h * R_s$

Then we fit a line to the IV data ($I_{m,compensated}$ vs. $V_{h,compensated}$) for the four holding potentials at each time point in the trace. The slopes and intercepts of these lines were used to calculate the total conductance g_T (the slope) and the reversal potential V_{rev} (-intercept/slope). We assumed that the excitatory reversal potential V_e = 0 mV and calculated the inhibitory reversal potential V_i = -73 mV based on the ionic compositions of our external and internal solutions. Then, the following equations were used to calculate the excitatory (g_e) and inhibitory (g_i) conductances as a function of time (t):

(3) $g_i(t) = \frac{g_T(t)*(V_{rev}(t)-V_e)}{V_i-V_e}$

(4) $g_e(t) = g_T(t) - g_i(t)$

For Fig. 2, 4C-D, S2, S4, S5, we quantified the resulting conductance traces with respect to the light spot stimulus during two time periods by integrating over an 800 ms time window from 50-850 ms after light onset and from 100-900 ms after light offset. Tonic responses in Fig. S3 were measured by integrating over the time period from 1050 to 1850 ms after light onset. For Fig. 3C-D, 4F, 5A and G, 6C and S6, we quantified the charge transfer by integrating over the excitatory current recorded at -72 mV in the same time windows. We chose these specific time windows based on the population response onset and duration.

Analysis of the experiments in Fig. 3B-C, 4E-F and Fig. 5B-G were performed in IgorPro (Wavemetrics, Inc) using NeuroMatic functions. Five sweeps at each condition were averaged. For Fig. 5F-G, charge transfer was calculated by integrating over the 400 ms following the time of the maximum current. For Fig. 5C and E, the variance was

calculated from 5 raw current sweeps (unaveraged) over two 1800 ms time windows when the light is off (100-1900 ms from beginning of the recording) and when the light was on (100-1900 ms after light onset). Then we calculated the average variance of the 5 current sweeps for five different cells.

For calcium imaging, images were analyzed offline using custom MATLAB software. The regions of interest (ROIs) of cells were determined using the Trainable Weka Segmentation (Waikato Environment for Knowledge Analysis) (Fiji) on all cells in a field-of-view, and the pixel intensities within an ROI were averaged at each time step. The fluorescence intensity of a neuron is reported throughout as the average intensity of all pixels over its soma, including the nucleus. The mean intensity value for each cell was filtered with a rolling ball filter to eliminate any wandering baseline. Fluorescence responses are reported as normalized increases as follows:

$$\frac{\Delta F}{F} = \frac{F - F_{\circ}}{F_{\circ}}$$

where F is instantaneous fluorescence induced by UV light stimulation and F_o is the baseline fluorescence when visual stimulation is absent.

The directionally selective index (DSI) was calculated for the two-photon OGB-1 signals as:

$$DSI = \frac{\frac{\Delta F}{F}_{pref} - \frac{\Delta F}{F}_{null}}{\frac{\Delta F}{F}_{pref} + \frac{\Delta F}{F}_{null}}$$

Where $[\Delta F/F]_{pref}$ and $[\Delta F/F]_{null}$ are the mean amplitudes of [ΔF/F] evoked by the bars moving in the preferred and null directions, respectively. The preferred direction of the cells was indicated by the direction of the vector sum of [ΔF/F] to all directions. The null

direction was 180 degree rotated from preferred. The trial-averaged values are given as the mean ± SD. Cells were considered direction selective if DSI>0.4.

Statistics

Unless otherwise stated in the Results, to compare between control and test populations, we ran a Wilcoxon rank-sum test in MATLAB. Significance levels of the difference between median values of the two populations are reported by the p value.

Simulation of changes in DSGCs' directional tuning following polarity switch in SACs

Excitatory and inhibitory conductances onto DSGCs in response to PD and ND grating stimulation were simulated as rectified sinusoids. For simplification, the simulation included responses mediated only by the On pathway. The relative timing between excitation and inhibition was changed to estimate the effect of a phase shift in the inhibitory conductance onto DSGCs on their directional preference. Excitatory conductance did not depend on the direction of stimulation, while inhibitory conductance in response to ND stimulation preceded inhibitory conductance in response to PD stimulation by half a cycle (π). This time difference between inhibitory conductance towards PD and ND stimulation remained constant throughout the simulation, and the inhibitory conductances in response to both directions were shifted together in the simulation.

Control state (un-adapted), was defined as 0 phase shift. Here, inhibition co-occurred with excitation and canceled out the excitation in response to ND stimulation

but not in response to PD stimulation. Inhibitory conductances were shifted from 0 phase to 2π phase, to cover all possible time shifts between excitatory and inhibitory conductances.

For each given phase shift, we determined the membrane potential of a DSGC in response to drifting gratings in each time point based on the excitatory and inhibitory conductances as follows:

(5) $V_m(0) = -60$

(6) $I(t+1) = g_{exc}(V_m(t) - 0) + g_{inh}(V_m(t) + 80)$

(7) $V_m(t) = V_m(t-1) - I(t) * R$

where $V_m(t)$ is the membrane potential at time t; $I(t)$ represents the total synaptic current to the cell at time t based on the excitatory and inhibitory conductances, g_{exc} and g_{inh}, and their reversal potentials, 0mV and -80mV, respectively; R is the input resistance of the DSGC, (estimated at 100 MOhm).

Spiking activity in the DSGC in response to PD and ND stimulation were randomly generated based on membrane potential values at each time point. Action potentials had a probability of 0 for membrane potentials lower than or equal to -40mV, and a probability of $(V_m(t)+60)/100$ for higher membrane potential values (e.g., $P_{spike}(t \mid V_m(t)=-20)=0.4$). For every phase shift, we generated 100 spike trains in response to PD and ND stimulation and calculated the direction selective index (DSI) for each pair based on:

(8) $DSI = < \frac{PD_i - ND_i}{PD_i + ND_i} >$

where PD_i and ND_i represent total number of spikes in the ith random spike trains in response to PD and ND stimulations, and <.> denotes averaging.

Briggman, K.L., and Euler, T. (2011). Bulk electroporation and population calcium imaging in the adult mammalian retina. J. Neurophysiol. *105*, 2601–2609.

Dalkara, D., Byrne, L.C., Klimczak, R.R., Visel, M., Yin, L., Merigan, W.H., Flannery, J.G., and Schaffer, D.V. (2013). In vivo-directed evolution of a new adeno-associated virus for therapeutic outer retinal gene delivery from the vitreous. Sci Transl Med *5*, 189ra76.

Deans, M.R., Volgyi, B., Goodenough, D.A., Bloomfield, S.A., and Paul, D.L. (2002). Connexin36 is essential for transmission of rod-mediated visual signals in the mammalian retina. Neuron *36*, 703–712.

Flannery, J.G., and Visel, M. (2013). Adeno-associated viral vectors for gene therapy of inherited retinal degenerations. Methods Mol. Biol. *935*, 351–369.

Huberman, A.D., Wei, W., Elstrott, J., Stafford, B.K., Feller, M.B., and Barres, B.A. (2009). Genetic identification of an On-Off direction-selective retinal ganglion cell subtype reveals a layer-specific subcortical map of posterior motion. Neuron *62*, 327–334.

Ivanova, E., Hwang, G.S., and Pan, Z.H. (2010). Characterization of transgenic mouse lines expressing Cre recombinase in the retina. Neuroscience *165*, 233–243.

Ivanova, E., Lee, P., and Pan, Z.-H. (2013). Characterization of multiple bistratified retinal ganglion cells in a purkinje cell protein 2-Cre transgenic mouse line. J. Comp. Neurol. *521*, 2165–2180.

Rivlin-Etzion, M., Wei, W., and Feller, M.B. (2012). Visual stimulation reverses the directional preference of direction-selective retinal ganglion cells. Neuron *76*, 518–525.

Taylor, W.R., and Vaney, D.I. (2002). Diverse synaptic mechanisms generate direction selectivity in the rabbit retina. J. Neurosci. *22*, 7712–7720.

Watanabe, D., Inokawa, H., Hashimoto, K., Suzuki, N., Kano, M., Shigemoto, R., Hirano, T., Toyama, K., Kaneko, S., Yokoi, M., et al. (1998). Ablation of Cerebellar Golgi Cells Disrupts Synaptic Integration Involving GABA Inhibition and NMDA Receptor Activation in Motor Coordination. Cell *95*, 17.

Wei, W., Elstrott, J., and Feller, M.B. (2010). Two-photon targeted recording of GFP-expressing neurons for light responses and live-cell imaging in the mouse retina. Nat Protoc *5*, 1347–1352.